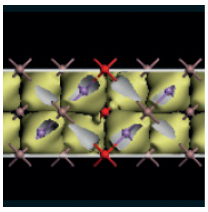

Density matrix model for bound to continuum terahertz quantum cascade lasers

A Demić[1], A Grier[2], Z Ikonić[1], A Valavanis[1], R Mohandas[1], L Li[1], E Linfield[1], A G Davies[1] and D Indjin[1]

[1]University of Leeds, UK, [2] Seagate Technology, UK

Terahertz-frequency quantum cascade lasers (THz QCLs) require very small energy difference between the lasing states (~10 meV), and modelling of these devices can be challenging. Furthermore, thermal excitation of carriers can rapidly degrade device performance and THz QCLs must operate at cryogenic temperatures. A variety of materials and approaches are being employed in order to improve the thermal performance of QCLs [1], and this must be underpinned by a good understanding of carrier transport within these devices. Various models for transport in QCLs exist [2]; most commonly employing semi-classical approaches such as self-consistent rate-equation (RE) modelling, which considers non-radiative transitions of carriers due to various scattering mechanisms, including interactions of electrons with phonons (LO), alloy disorder (AD), interface roughness (IRF), ionised impurities (II) and other electrons (CC). These models are semi-classical because they consider transitions of discrete electrons between energy levels and neglect coherence effects and quantum mechanical dephasing. Although RE models are usually computationally efficient, and provide insight into the scattering behaviour, they are unable to correctly describe transport between adjacent periods of a QCL structure [3] because they do not take injection barrier thickness into account in transport calculations. This leads to the prediction of instantaneous transport between the periods, whereas the actual transport that occurs is based on resonant tunnelling.

Alternative approaches, based on density matrix (DM) modelling include quantum transport effects and are able to overcome known shortcomings of RE models, while keeping reasonable computational complexity. DM models include a finite dephasing time through the barrier as well as Rabi oscillations at the frequency $\Delta ij'I\ \hbar$, where $\Delta ij'$ is the anticrossing energy between state i and j' where j' is the state from the adjacent period which is aligned with state i due to the external bias.

RE models can be successfully applied to mid infra-red (MIR) structures [4] which have much larger photon energies and due to the thin injection barriers anticrossing gaps are large (which causes fast oscillations through the barrier). However, THz QCLs strongly depend on the coherent transport and an appropriate model needs to be used.

DM models are frequently applied to approximate QCL bandstructure, containing just 2 or 3 states per period [5]. Although this approach reduces the computational complexity, it results in a cumbersome set of analytic expressions, which is inconvenient for bound-to-continuum (BTC) THz QCLs, since these have a large number of states per module.

In this work, we present a new DM approach that extends the model presented in [6], applicable for arbitrary number of states per module. This model has proved successful for a variety of QCL simulations, including BTC structures [7], quantum dot QCLs [8], non-linear effects [9] and self-mixing interferometry [10].

The time evolution of the density matrix is described by the Liouville equation. We consider QCL structure with infinite number of periods, which implies infinite-sized matrices, but due to the nearest neighbour approximation and symmetry of QCL structure Liouville equation folds into the following system of $N \times N$ block equations (where N is the number of states in the module):

$$\frac{d\rho_1}{dt} = -\frac{i}{\hbar}([H_1,\rho_1]+[H_3,\rho_2]+[H_2,\rho_3]) - \frac{\rho_1}{\tau} - \frac{\rho_1}{\tau_{||}}$$
$$\frac{d\rho_2}{dt} = -\frac{i}{\hbar}([H_2,\rho_1]+[H_1,\rho_2]+KL_P\rho_2) - \frac{\rho_2}{\tau_{||}}$$
$$\frac{d\rho_2}{dt} = -\frac{i}{\hbar}([H_3,\rho_1]+[H_1,\rho_3]-KL_P\rho_3) - \frac{\rho_3}{\tau_{||}}$$

The Hamiltonian block H_1 describes the central period and is composed of tight-binding energies (on the main diagonal) and optical coupling terms of the form $H_{ij} = ez_{ij}\,A_{\text{inc}}$ where z_{ij} are dipole matrix elements, and A_{inc} is the electric field of the incident light. In this work, we use the non-rotating-wave approximation (NRWA) presented in [6] and assume that optical field has the form $A_{\text{inc}} = A_0(e^{iwt} + e - i\omega t)$ and therefore refer to the main diagonal of H_1 as H^{dc}, while the remaining ac terms have equal amplitudes which represent H^{ac}, (where $H_{ij}^{ac} = e_{zij}\,A_0$).

Hamiltonian blocks H_2 and H_3 only have dc terms which implies that $H_2 = H_3$. The elements in H_2 and H_3 contain Rabi coupling terms (half the anticrossing energy over ħ), and formally these blocks are obtained by $\langle i|H_{TB} - H_{EXT}|j\rangle$, where H_{TB} EXT for Rabi coupling terms from [11], [12].

Transport terms τ and $\tau||$ correspond to intraperiod and interperiod transport respectively and account to pure dephasing as well. Term τ is obtained by semi-classical Fermi's golden rule, while $\tau||$ describes interperiod transport in coherent manner. This is the main difference between the RE and DM approaches: RE uses Fermi's golden rule for interperiod transport as well, while in DM we assume that resonant tunnelling will occur at the Rabi frequency through the injection barrier, which is described by the Hamiltonian blocks H_2 and H_3, and that states additionally change their phase during the interperiod transport. Output of the system (current density and gain) are calculated as:

$$j = \frac{ien_{2D}}{\hbar L_P}\mathrm{Tr}\left(\rho_1[H_1,Z]+\rho_2[H_3,Z]+\rho_3[H_2,Z]+L_P(H_2\rho_3-\rho_2H_3)\right)$$
$$g = -\frac{we\,n_{2D}}{\varepsilon_0 A_0 n_r c\hbar}\mathrm{Tr}\left(\rho_1^{AC}Z\right)$$

We apply the model to the structure similar to one in [13]. The structure is designed for emission at 2.06 THz at 20K. The current-voltage I–V characteristic of the device can be calculated by sweeping the applied electric field (terminal voltage).

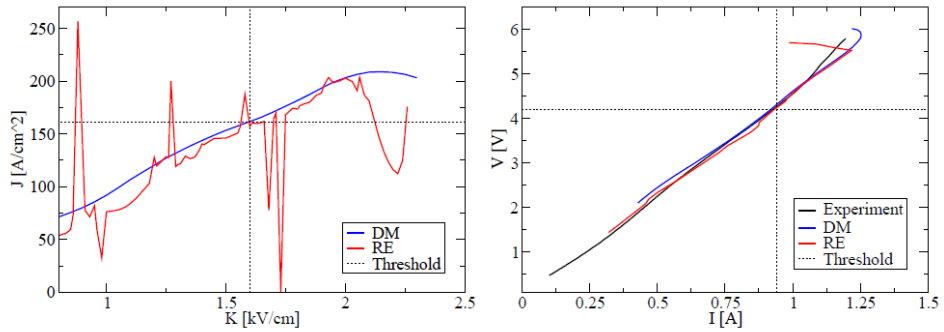

Fig. 1. **a)** Current density versus electric field from RE (red) and DM model (blue). Results were fitted to threshold point at $(K_t, J_t) = (1.6\ \mathrm{kV/cm}, 161.5\ \mathrm{A/cm^2})$ and **b)** I-V characteristic of the BTC device at 20K. RE model fit (red) needed 2.72 Ω of contact resistance, while DM model fit (blue) neede 2.25 Ω of contact resistance, both results were fitted to experimental threshold at $(I_t, V_t) = (0.94\,\mathrm{A}, 4.2\,\mathrm{V})$.

Density matrix results show a smooth dependence in Fig. 1, while RE model exhibits non-physical spikes. In order to obtain comparison with experimental current–voltage (I–V) characteristics, the axes in Fig. 1 b) need to be scaled by the corresponding device dimensions, but an additional fitting parameter is also required. In order to fit theoretical data to the experiment, non-zero contact resistance needs to be included in the model, this resistance is usually not known from the experimental setup, but it is reasonable to assume the values of several Ohms. Figure 1 b) shows how RE and DM model compare to the experimental output, note that here we manually removed the spikes that occurred in Fig. 1 a) while this is not necessary for the DM model, this property shows promise for application in QCL devices optimisation.

[1] S. Kumar, “Recent Progress in Terahertz Quantum Cascade Lasers,” IEEE Journal of Selected Topics in Quantum Electronics, vol. 17, no. 1, pp. 38–47,2011.
[2] C. Jirauschek and T. Kubis, “Modeling techniques for quantum cascade lasers,” Applied Physics Reviews, vol. 1, no. 1, p. 011307, 2014.
[3] H. Callebaut and Q. Hu, “Importance of coherence for electron transport in terahertz quantum cascade lasers,” Journal of Applied Physics, vol. 98,no. 10, p. 104505, 2005.
[4] D. Indjin, P. Harrison, R. W. Kelsall, and Z. Ikonic, “Self-consistent scattering model of carrier dynamics in GaAs-AlGaAs terahertz quantum-cascade lasers,” IEEE Photonics Technology Letters, vol. 15, no. 1, pp. 15–17, 2003.
[5] R. W. Boyd, Nonlinear Optics. Academic Press, 2008.
[6] T. V. Dinh, A. Valavanis, L. J. M. Lever, Z. Ikoni´c, and R. W. Kelsall, “Extended density-matrix model applied to silicon-based terahertz quantum cascade lasers,” Phys. Rev. B, vol. 85, no. 23, p. 235427, 2012.
[7] A. Grier, Modelling the optical and electronic transport properties of AlGaAs and AlGaN intersubband devices and optimisation of quantum cascade laser active regions. Phd, University of Leeds, 2015.
[8] B. A. Burnett and B. S. Williams, “Density matrix model for polarons in a terahertz quantum dot cascade laser,” Phys. Rev. B, vol. 90, no. 15, p. 155309, 2014.
[9] B. A. Burnett and B. S. Williams, “Origins of Terahertz Difference Frequency Susceptibility in Midinfrared Quantum Cascade Lasers,” Phys. Rev. Applied, vol. 5, no. 3, p. 034013, 2016.
[10] A. Grier, P. Dean, A. Valavanis, J. Keeley, I. Kundu, J. D. Cooper, G. Agnew, T. Taimre, Y. L. Lim, K. Bertling, A. D. Raki´c, L. H. Li, P. Harrison, E. H. Linfield, Z. Ikoni´c, A. G. Davies, and D. Indjin, “Origin of terminal voltage variations due to self-mixing in terahertz frequency quantum cascade lasers,” Opt. Express, vol. 24, no. 19, pp. 21948–21956, 2016.
[11] A. Yariv, C. Lindsey, and U. Sivan, “Approximate analytic solution for electronic wave functions and energies in coupled quantum wells,” Journal of Applied Physics, vol. 58, no. 9, pp. 3669–3672, 1985.3
[12] G. Bastard, Wave Mechanics Applied to Semiconductor Heterostructures. EDP SCIENCES, 1988.
[13] J. R. Freeman, O. Marshall, H. E. Beere, and D. A. Ritchie, “Improved wall plug efficiency of a 1.9 thz quantum cascade laser by an automated design approach,” Applied Physics Letters, vol. 93, no. 19, p. 191119, 2008.